J Neurophysiol 93: 2104–2116, 2005.
First published November 10, 2004; doi:10.1152/jn.00601.2004.

Temporal Dynamics of Direction Tuning in Motion-Sensitive Macaque Area MT

János A. Perge, Bart G. Borghuis, Roger J. E. Bours, Martin J. M. Lankheet, and Richard J. A. van Wezel
Functional Neurobiology, Helmholtz Institute, Faculty Biology, Utrecht University, Utrecht, The Netherlands

Submitted 14 June 2004; accepted in final form 3 November 2004

Perge, János A., Bart G. Borghuis, Roger J. E. Bours, Martin J. M. Lankheet, and Richard J. A. van Wezel. Temporal dynamics of direction tuning in motion sensitive macaque area MT. *J Neurophysiol* 93: 2104–2116, 2005. First published November 10, 2004; doi:10.1152/jn.00601.2004. We studied the temporal dynamics of motion direction sensitivity in macaque area MT using a motion reverse correlation paradigm. Stimuli consisted of a random sequence of motion steps in eight different directions. Cross-correlating the stimulus with the resulting neural activity reveals the temporal dynamics of direction selectivity. The temporal dynamics of direction selectivity at the preferred speed showed two phases along the time axis: one phase corresponding to an increase in probability for the preferred direction at short latencies and a second phase corresponding to a decrease in probability for the preferred direction at longer latencies. The strength of this biphasic behavior varied between neurons from weak to very strong and was uniformly distributed. Strong biphasic behavior suggests optimal responses for motion steps in the antipreferred direction followed by a motion step in the preferred direction. Correlating spikes to combinations of motion directions corroborates this distinction. The optimal combination for weakly biphasic cells consists of successive steps in the preferred direction, whereas for strongly biphasic cells, it is a reversal of directions. Comparing reverse correlograms to combinations of stimuli to predictions based on correlograms for individual directions revealed several nonlinear effects. Correlations for successive presentations of preferred directions were smaller than predicted, which could be explained by a static nonlinearity (saturation). Correlations to pairs of (nearly) opposite directions were larger than predicted. These results show that MT neurons are generally more responsive when sudden changes in motion directions occur, irrespective of the preferred direction of the neurons. The latter nonlinearities cannot be explained by a simple static nonlinearity at the output of the neuron, but most likely reflect network interactions.

INTRODUCTION

In visual motion analysis, local motion signals have to be integrated into globally meaningful motion signals. This requires effective spatial and temporal summation of comparable motion signals, especially in a visual environment with low signal-to-noise ratio. On the other hand, the brain should also detect and process spatio-temporal differences in motion. Detection of differences in the direction or speed of motion is critically important in figure-background segregation, object localization, or breaking camouflage. Because requirements for efficient integration essentially differ from those for detecting motion differences, one could expect that brain areas involved in motion processing contain motion detectors that integrate or differentiate motion signals.

In primates, the middle temporal area (area MT or V5) plays an important role in motion perception (Britten et al. 1996; Newsome and Paré 1988; Salzman et al. 1992). Neurons in area MT respond selectively to a particular subset of directions and speeds of motion within their receptive field (Albright 1984; Dubner and Zeki 1971; Maunsell and Van Essen 1983; Mikami et al. 1986). Numerous studies have established a close link between processes of integration/segregation in motion perception and the response characteristics of MT neurons (Britten and Heuer 1999; Britten and Newsome 1998; Britten et al. 1992; Buracas et al. 1998; Heuer and Britten 2002; Movshon et al. 1985; Pack and Born 2001; Pack et al. 2004; Rudolph and Pasternak 1999; Snowden et al. 1991; Treue et al. 2000). Directional interactions underlying motion segregation and integration have been studied extensively in MT neurons. Most of these studies concerned simultaneous spatial interactions between different parts of the receptive field and showed that MT neurons differ with respect to the degree of spatial segregation and integration. For instance, for a subset of MT neurons, the response to the preferred direction in the receptive field center is suppressed by the same direction in the surrounding area (Allman et al. 1985; Born 2000; Born and Tootell 1992; Raiguel et al. 1995; Xiao et al. 1995). This phenomenon, often referred to as center-surround antagonism, makes neurons with strong antagonistic surrounds excellent candidates for playing an important role in spatial segregation of differently moving objects. Other MT neurons either lack surrounds or have reinforcing surrounds and integrate motion over large areas of the visual field to encode information about global motion. Other studies showed different degrees of motion integration for stimuli presented at different positions within the receptive field center (Movshon et al. 1985; Pack and Born 2001; Rodman and Albright 1989). These studies reveal that when MT neurons are stimulated by plaids containing multiple motion components, some neurons respond to the separate components, whereas others, the so-called "pattern neurons", respond to the global pattern.

Center-surround antagonism and component/pattern selectivity indicate how the spatial receptive field organization of MT neurons contributes to the integration or segregation of simultaneous motion cues. On the other hand, the temporal aspects of motion integration and segregation in area MT have received less attention. Recent work by Priebe and colleagues. (Priebe and Lisberger 2002; Priebe et al. 2002) showed that MT neurons show different degrees of short-term motion adaptation, which would make them differentially sensitive to temporal motion contrast. They also showed specific temporal interactions between stimuli in the preferred and in the antipreferred direction. When two motion directions are presented consecutively, the response to the second stimulus is sup-

Address for reprint requests and other correspondence: R. van Wezel, Functional Neurobiology, Faculty Biology, Utrecht Univ., Padualaan 8, 3584 CH Utrecht, The Netherlands (E-mail: r.j.a.vanwezel@bio.uu.nl).

The costs of publication of this article were defrayed in part by the payment of page charges. The article must therefore be hereby marked "*advertisement*" in accordance with 18 U.S.C. Section 1734 solely to indicate this fact.

pressed if the preceding stimulus moves in the preferred direction and either enhanced or suppressed if the preceding stimulus moves in the antipreferred direction.

One problem with addressing the topic of temporal motion integration and segregation is that it has been difficult to isolate the response to single motion steps, which form the basic signals on which segregation and integration processes act. Whenever multiple motion steps in the same direction are used, the basic response to individual stimuli is confounded by effects of temporal integration and/or associated adaptation. Recently, we introduced a motion reverse correlation paradigm, which allows us to study the basic response of MT neurons to individual stimuli (Borghuis et al. 2003). In this paradigm, stimuli consisted of a sequence of motion steps in random directions. Reverse correlation of spike occurrences and motion steps reveals the time course of relative responses to single motion steps in different directions. The method also offers the possibility to analyze responses to consecutive steps and study directional interactions in time.

The purpose of this paper was to study the temporal, rather than the spatial aspects of motion integration and segregation in area MT using the motion reverse correlation method. We are focusing on two questions. First, to what extent do MT neurons differ in their time course of responses to single motion steps at their preferred speed? Second, what is the effect of consecutive motion steps in different motion directions? We found different types of responses to single motion steps, showing different degrees of temporal integration and segregation. Responses to consecutive motion steps show that the increased sensitivity of MT neurons to opposite directions is not limited to the antipreferred/preferred combination, but increased sensitivity can also be found for other near opponent combinations of directions. These special nonlinear effects may be due to specific network interactions. Because interactions are quantified at high temporal resolution (in the order of milliseconds), they provide important clues to the structure of the underlying network of motion detectors.

METHODS

Two adult male rhesus macaques (*Macaca mulatta*) participated in this study. Before the experiments, each monkey was implanted surgically with a head holding device, a search coil for measuring eye movements using the double induction technique (Malpeli 1998; Reulen and Bakker 1982), and a stainless steel recording cylinder placed over a craniotomy above the left occipital lobe. The surgical procedures were performed under N_2O/O_2 anesthesia supplemented with isoflurane. After recovery, the monkeys were trained to fixate a rectangular spot ($0.4 \times 0.4°$) on a black background. During the experiments, each monkey sat in a primate chair 57 cm from a cathode-ray tube display. Eye movement recordings were sampled at 500 Hz. For accurate fixation, the monkeys had to maintain their viewing direction within a virtual fixation window around the fixation point (2° diam). While correctly fixating, the monkey was rewarded with water or juice every 3 s. Breaking fixation resulted in pausing the presentation of stimuli and lack of a reward. Stimulus presentations were restarted after 300 ms of correct fixation. Animal procedures used in this study were approved by the Animal Use Committee (DEC) of Utrecht University, and procedures were according to national and international guidelines.

Neuronal recordings

During experimental sessions, a parylene-insulated Tungsten microelectrode (0.5–2 MΩ at 1 kHz) was inserted manually through a guide tube and manipulated by a micropositioning controller. Area MT was identified by the recording position and depth, by the transition between gray matter, white matter, and sulci along the electrode track, and by its functional properties. These are, among others, the prevalence of direction selective units, the similarity in direction tuning for nearby single unit recordings, the receptive field size according to eccentricity and the change of direction tuning along the electrode penetration. We have no histological confirmation of the recording sites because both monkeys are currently being used in other experiments. Single unit recordings were carried out using standard extracellular methods. Spike times were registered with 0.5-ms resolution for on-line analysis and data storage, using a Macintosh G4 computer with National Instruments PCI 1200 data acquisition board.

Stimuli and experimental procedure

The monitor (Sony Trinitron Multiscan 500 PS) was driven by an ATI Rage graphics card. The refresh rate was 75 Hz (1152×870 pixels) for early experiments in monkey A (42% of 114 cells recorded in monkey A) and 120 Hz (1024×768 pixels) in the other experiments. The stimulus was a high-density binary random dot pattern in a rectangular field ($14 \times 14°$), consisting of 50% black and 50% white dots and surrounded by a black background (Julesz 1971). Mean luminance of the stimulus was 48 cd/m^2. A dot size of $0.14 \times 0.14°$ was used for 42% of the cells in monkey A and $0.20 \times 0.20°$ was used for all remaining cells.

The dot pattern was positioned over the receptive field center as determined by hand mapping. The dot pattern was shifted each monitor frame (8.3 ms at 120 Hz and 13.3 ms at 75 Hz) or every second monitor frame (17 ms at 120 Hz and 27 ms at 75 Hz). The size of the shift ranged between 0.07 and 0.42° (in steps of 0.07°) optimized for each cell to elicit the most activity. The shifts occurred in any of eight directions (from 0 to 315°, in steps of 45°, where 0° corresponds to rightward motion and 90° to upward motion) in a pseudo-random order. Each motion step was presented 700–1400 times in a randomized order. A movie demonstration of the direction tuning stimulus can be also viewed at our website[1]. Stimulus generation, data collection, and monitoring of the monkeys' performance was done with custom software written in programming language C. Off-line data analysis was done in MATLAB.

Data analysis

Stimulus generation and data analysis were performed using the motion reverse correlation method previously described elsewhere (Borghuis et al. 2003). Note that our stimulus is different from luminance contrast reverse correlation methods (e.g., Cook and Maunsell 2004; DeValois et al. 2000; Livingstone et al. 2001), in which motion selectivity is computed from a second-order analysis of the response to dynamically positioned stationary dots (or bars) at different locations in the receptive field. Since we use full field motion steps, in our method the stimulus is much more effective in eliciting spikes, which facilitates a detailed analysis of the response to consecutive motion steps. In our method, reverse correlograms were computed for each motion direction by reverse correlating the occurrence of motion steps with the spike train. Reverse correlograms for each

[1] The Supplementary Material (a movie) is available online at http://jn.physiology.org/cgi/content/full/00601.2004/DC1.

direction were converted to relative probabilities by dividing the number of stimulus occurrences at each prespike time by the total number of stimuli at that time. Values for each stimulus, normalized in this way, range from 0 to 1, where 0 indicates zero relative probability for a given stimulus to occur at that time before a spike and a value of 1 indicates perfect correspondence (each spike preceded by a given stimulus at the specified time before a spike).

The value of equal probability (the baseline of the reverse correlograms) corresponds to a level of $1/n$, where n is the number of stimuli in the set. In our experiments, eight different directions resulted in an equal probability level of 0.125. Note that the equal probability level is not identical to spontaneous activity. This value indicates that the effect of a particular stimulus is similar to the mean effect across the whole set of stimuli.

Our results would be identical whether correlating the stimuli to the spikes (reverse correlation) or the spikes to the stimuli (forward correlation). However, the main reason to use reverse correlation in this study was that our stimulus consists of motion impulses with very short intervals (8–24 ms). Therefore the correlogram is not only the average effect of one specific stimulus, but also the average effect of the preceding and following stimuli that were used. If we presented our data in conventional stimulus-response histograms, one could get the false impression that the responses were only the result of one particular stimulus.

The reverse correlograms obtained for the individual directions are not independent. Since we use a limited set of motion directions, we only obtained information on relative probability levels. An increased probability for one direction inevitably leads to a decreased probability level for the other directions. As a result, we cannot differentiate between excitatory effect for one stimulus direction and simultaneous inhibitory effect for another one. Moreover, the choice of stimuli might affect reverse correlograms obtained for a specific response. However, for direction experiments, as we report in this study, the tuning properties were found not to depend on the number of directions, as long as they were properly balanced. Borghuis et al. (2003) analyzed the effect of the number of directions in a single experiment on direction tuning. They found that, although the absolute probability values changed, there were no significant differences between tuning curves obtained with 4, 8, and 16 directions, except for the obvious increase in sampling resolution.

In most cases, one is not primarily interested in the raw correlation values, but rather the statistical significance of those correlations. The noise level of the correlograms may fluctuate with the mean firing rate and with the total length of a measurement. Noise levels therefore differ between cells and between measurements. We estimated the noise level in each recording by analyzing a time period of 100 ms following spikes. Because stimuli occurring after a spike cannot have any effect on its occurrence, deviations from chance level in this part of the correlogram are by definition uncorrelated and reflect the noise in the correlogram. The noise level was quantified by the SD relative to the equal probability level, for all stimuli together. We used an arbitrary level of 3 SD for defining significant excursions in the reverse correlograms. The chance that reverse correlograms surpassed this level spontaneously was very small.

The reverse correlogram with the highest probability value corresponds to the preferred direction, whereas the stimulus direction 180° away from the preferred direction is defined as the antipreferred direction. In nearly all cases, antipreferred reverse correlograms also had the lowest probability values. As shown in an earlier publication (Borghuis et al. 2003), the preferred direction determined with this reverse correlation technique is in accordance with preferred direction measured with hand-mapping techniques or conventional stimuli (moving random dot patterns and gratings).

The large number of stimulus repetitions also allows us to study temporal interactions between stimuli. To this end, we computed the correlation between spikes and combinations of successive motion directions. This analysis can reveal interactions between a specific combination of motion directions, as well as the time course of such interactions. This second-order reverse correlation is similar to the first-order correlation described above, except that each direction is subdivided in eight subclasses, one for each motion direction preceding the stimulus. Second-order reverse correlation thus results in 64 correlograms describing direction combination occurrences as a function of prespike time. In our second-order analysis, the first and second stimuli occurred successively. However, it is also possible to obtain correlograms for motion steps that are separated by one or several others. As a convention, we used the occurrence of the last motion step in the sequence as *time 0* in the correlogram.

First-order and second-order reverse correlograms were smoothed by sliding window averaging with a Gaussian profile. We used an SD of 8 ms, which was found to remove most of the noise without affecting the overall shape of the function and its main parameters.

To link the temporal profile of reverse correlograms to the temporal profile of responses to long duration stimulation, we performed an additional measurement. After measuring the direction tuning curves of 31 neurons with the reverse correlation technique, we also recorded the responses to continuously moving random dot patterns. The dot patterns were presented in the preferred direction for a duration of 1 s and were repeated 10 times. Other parameters of the stimulus such as speed, dot size, and pattern size were identical to the motion reverse correlation stimulus. Post-stimulus time histograms (PSTHs) with a bin-width of 10 ms were computed, and the time course of the histograms was further analyzed (see RESULTS).

RESULTS

Motion direction tuning curves were measured with the reverse correlation technique at the preferred step size of MT neurons (see METHODS) of two male rhesus macaque monkeys for a total of 169 neurons (114 neurons in monkey A and 55 in monkey S). First we will describe the temporal dynamics of direction tuning in MT neurons, based on individual motion steps. Next, we will analyze the effect of specific combinations of motion directions, and finally, we will show how these results differ from the predictions based on tuning to individual steps.

Temporal dynamics of direction tuning

Reverse correlograms for the eight motion directions are shown for two typical example cells in Fig. 1, *A* and *B*. Direction tuning curves can be obtained at each point in time, based on the correlograms for the eight different directions. Three examples of these polar direction tuning plots, at different prespike times, are shown as *insets* in Fig. 1, *A* and *B*. The complete temporal profile of direction tuning for these two neurons is shown in a polar plot movie at our website (http://www-vf.bio.uu.nl/lab/NE/publications/JP/results.html).

Another way to present the time course of direction tuning is to calculate directional vector sums based on the eight reverse correlograms at each moment in time. For this calculation, the length of the vectors is the probability value of the vector sum of the eight correlograms. The direction of the vector sum is upward for a vector sum in the preferred direction and downward for the null direction. Figure 1, *C* and *D,* shows the vector sum representation for each point in time for the example cells in Fig. 1, *A* and *B*, respectively. Vector sums calculated in this way provide a good summary of preferred direction and

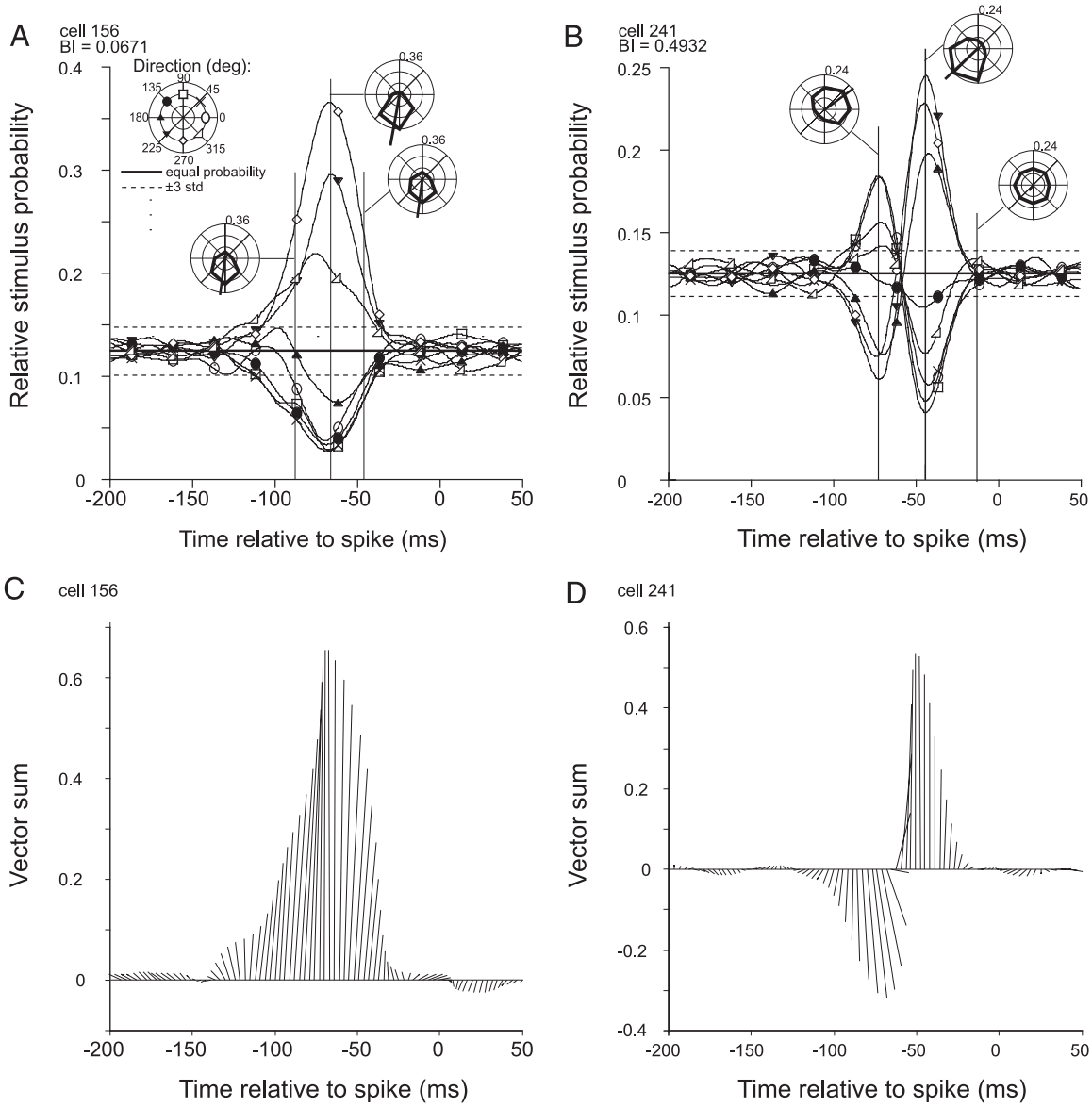

FIG. 1. Time course of direction tuning in MT neurons reveals different response behaviors. *A*: neuron without biphasic behavior. *B*: neuron with strong biphasic behavior. The 8 reverse correlogram curves represent relative probability of each stimulus direction before action potentials. Symbols indicate the motion direction (see *inset*). *Time 0* represents spike occurrences. Solid horizontal line indicates equal probability. Two horizontal dashed lines indicate 3 SD above or below equal probability. Three polar plots indicating relative probabilities for certain directions are inserted at 3 time stamps. Origin of polar plots is a probability of 0, and maximum value is indicated on *top* of the polar plot. Vector sum of these probabilities is indicated by a thick oriented line in the polar plot. A polar plot movie showing the complete temporal progress of the direction tuning can be viewed at our website (http://www-vf.bio.uu.nl/lab/NE/publications/JP/results.html). Directional vector sums of the 8 reverse correlograms show the average stimulus as a function of time before the spikes. *C*: directional vector sums of a neuron without biphasic behavior (same neuron as *A*). *D*: directional vector sums of a neuron with strong biphasic behavior (same neuron as *B*). Longer vectors indicate stronger direction tuning. Direction of vector sums are up for the preferred direction and down for the antipreferred direction.

strength of directional selectivity (vector length) as a function of time.

The two example cells in Fig. 1 show the variability in the shape of the reverse correlograms among the recorded MT neurons. The example in Fig. 1*A* shows, for each direction, only a single phase, which is either positive or negative, whereas the example in Fig. 1*B* reveals two distinct temporal phases, one at short latency and another one with reversed polarity at a longer latency. We will refer to this temporal characteristic as *biphasic behavior*. To characterize the level of biphasic behavior over the whole population we computed for each cell a biphasic index

$$\text{Biphasic Index} = \frac{\text{maximum excursion of the antipreferred reverse correlogram from the equal probability level}}{\text{maximum excursion of the preferred reverse correlogram from the equal probability level}} \quad (1)$$

The biphasic index thus expresses the ratio between the maximum excitatory effect of preferred and antipreferred stimuli (*Eq 1*). Those two maxima are at different points in time (see Fig. 1*B*). A

low biphasic index value corresponds to lack of biphasic behavior (Fig. 1*A*) and a high value to strong biphasic behavior (Fig. 1*B*). Figure 2 shows the distribution of biphasic index values across the population of recorded MT neurons. The mean biphasic index for all of the cells was 0.19 ± 0.14 (n = 169). As Fig. 2 shows, the distribution of biphasic behavior for the population forms a unimodal distribution.

The example cell in Fig. 1*B* shows a reversal of optimal direction. At a latency of about 45 ms, the correlogram shows its maximum, corresponding to the cell's preferred direction. At a latency of about 70 ms, however, the directional preference is changed by about 180°. To characterize the directional change for the strongly biphasic neurons, we calculated the difference in vector direction between the two phases. For this analysis, we chose 25% of the neurons with the highest biphasic index (n = 42). Figure 3*A* shows the distribution of direction differences between the two peaks in the biphasic profiles (measured in the clockwise direction). On average, the change in direction was 170 ± 25°. Most cells show a directional difference of about 180°, i.e., a direction reversal.

To further characterize the time course of directional changes, we summarized the change in time for 25% of the neurons with the highest biphasic index. This analysis allows us to find out whether changes in the direction tuning take place through gradual rotations or by 180° direction reversals. Gradual changes would indicate contributions from multiple directions with different temporal dynamics, whereas direction reversals indicate a change in balance between preferred and antipreferred direction in time. To distinguish between these two possibilities, we averaged the directional vector sums of the strongly biphasic neurons. Directional vector sums along the entire time window were expressed as absolute deviations from the preferred direction (the preferred direction was defined as the vector sum at the peak latency of the phase with the shortest latency). Averaging absolute deviations from the preferred direction avoids possible cancellation of rotations in opposite directions for different neurons. We also normalized the time scale of each recording to the time difference between the two phases in the correlogram. In this way, individual differences in the dynamics of directional changes did not affect the average vector sum. Figure 3*B* shows the resulting time-normalized, average vector sum. The average vector sum did not show any sign of gradual rotation, but rather a distinct, abrupt shift from antipreferred to preferred direction. The balance between preferred and antipreferred directions changed in time, but there was no change in contribution from directional components different from the preferred/antipreferred axis.

The temporal dynamics of the correlograms for different directions were very similar. The differences in peak latencies

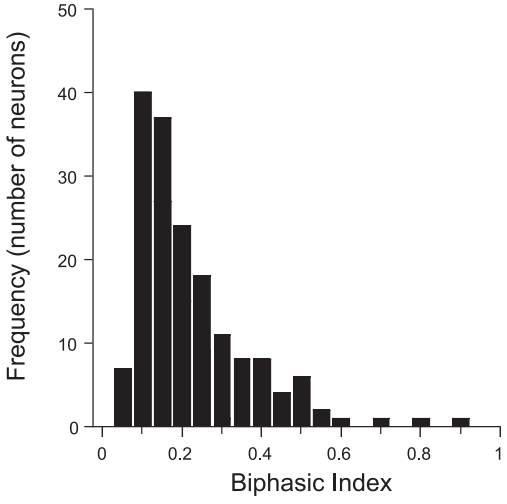

FIG. 2. Degree of biphasic behavior varies in the population. Frequency distribution of the biphasic index over the population (see *Eq. 1*). A biphasic index of 0 means complete lack of biphasic behavior. Two outliers are not shown in this graph. Average biphasic index was 0.19 ± 0.14 (n = 169).

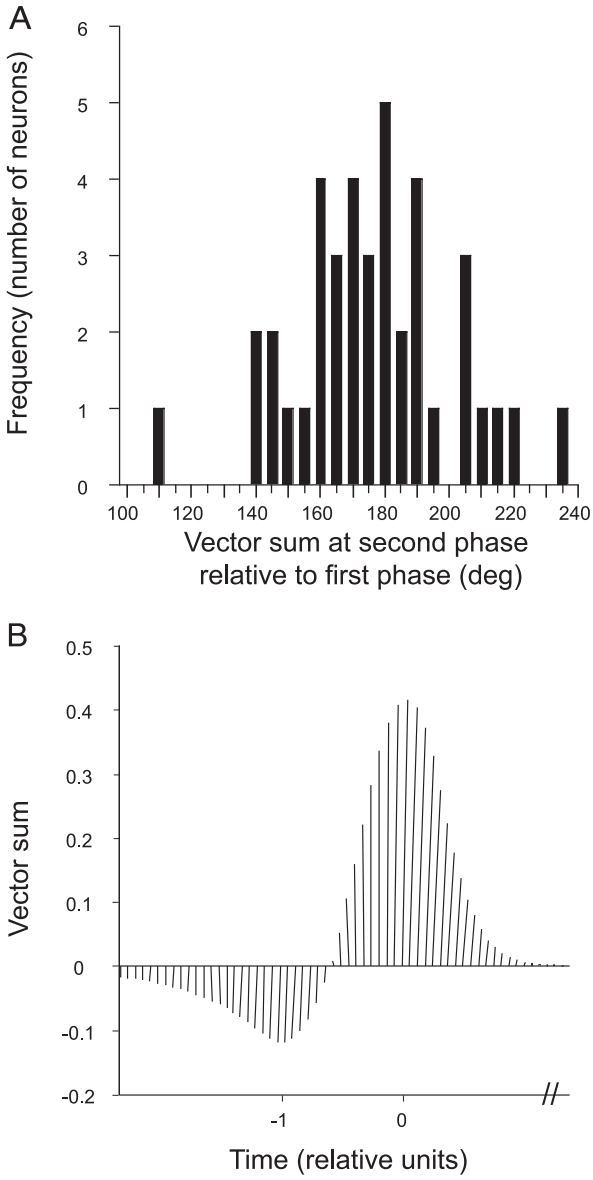

FIG. 3. Temporal change in direction tuning of strongly biphasic neurons (25% of neurons with highest biphasic index). *A*: distribution of angular differences between directional vector sums at the 1st and 2nd phase. Average difference was 170 ± 25°. Three outliers are not shown in this plot. *B*: directional vector sums as a function of time averaged over strongly biphasic neurons. Vector direction and length indicate average stimulus direction and tuning strength in Cartesian coordinates. Longer vectors indicate stronger direction tuning. Directions up and down represent the preferred and antipreferred directions, respectively. *Time 0* and *−1* represent peak latency of the 1st and 2nd phase, respectively.

TABLE 1. *Quantitative analysis of the temporal response profile. Definitions of parameters are explained in the schematic diagram next to the table. A weakly and strongly biphasic group was selected by taking 25% (n = 42) of the whole population of neurons with the lowest and 25% with the highest biphasic index respectively. All parameters are calculated for the preferred direction only. The peak latency (PL) and the rebound (RB) were at the latency of the highest and lowest probability values respectively. The first and last significant responses (FSS and LSS respectively) were obtained by starting at PL and stepping back and forth along the time axis until the first and last points were reached where the probability values were still higher than the equal probability level plus three standard deviations. The standard deviation of the noise was calculated for each neuron separately for a 100 ms section of the reverse correlograms after the spike occurrences for all eight directions. The last biphasic response (LBR) was the last significantly low value (where the correlogram was still less than equal probability minus 3 standard deviations). FSS, PL, and LSS were computed for all of the cells, and the remaining parameters were computed only for the strongly biphasic neurons. Using these 5 parameters four duration values (W1, W2, W3, and Δt) were calculated as indicated in the schematic diagram*

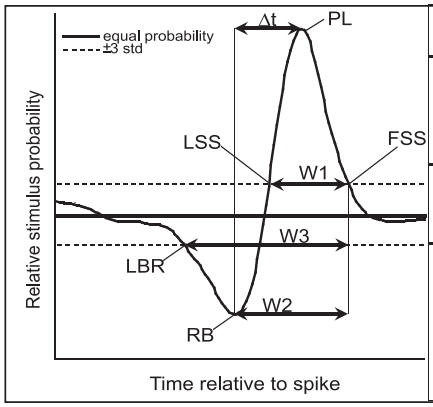

		Mean + SD ms	r
Total population (n = 169)	FSS	34 ± 9	0.10
	PL	58 ± 10	-0.13
	W1	47 ± 14	-0.26**
	Spike counts	1715 ± 1501	-0.01
Monophasic (n = 42)	FSS	35 ± 11	-0.07
	PL	60 ± 12	-0.12
	W1	54 ± 14	-0.33*
Biphasic (n = 42)	FSS	35 ± 8	0.17
	PL	56 ± 8	0.05
	Δt	38 ± 20	-0.06
	W1	40 ± 8	-0.27
	W2	59 ± 22	-0.10
	W3	62 ± 42	-0.06

The value 'r' indicates the correlation coefficient between biphasic index and the different parameters. The asterisks indicate significance levels of $P < 0.05$ (*) and $P < 0.01$ (**) respectively. No asterisk indicates a significant level of $P > 0.05$.

of the first phase (i.e., the largest excursion of the correlogram from the equal probability level) between the preferred direction and other directions were on average 1 ± 10 ms. There was no statistically significant difference between the peak latencies of the different directions in the population (1-way ANOVA, $F = 0.7$, $P = 0.67$). In 25% of the neurons with the highest biphasic index ($n = 42$), the average difference in peak latency of the second phase was −1 ± 9 ms, with no statistical difference (1-way ANOVA, $F = 0.33$, $P = 0.93$).

We analyzed in more detail the relationship between the biphasic index and the shape of the reverse correlogram and other response properties (as summarized in Table 1). Table 1 shows a summary of statistics for several temporal parameters for the whole population for the 42 (25%) most weakly biphasic cells and for the 42 most clearly biphasic cells. The last column shows the correlation coefficient with the biphasic index. Significant correlations are marked by single ($P < 0.05$) or double ($P < 0.01$) asterisks.

As shown in Table 1, the average peak response latency (PL) of the preferred direction for all neurons was 58 ± 10 ms, which is similar to response latencies reported previously based on pseudorandom temporal sequences of preferred and antipreferred stimuli (Bair et al. 2002). Peak latencies did not vary systematically with the biphasic index value in either group. The total width of the profile was on average 54 ms for weakly biphasic cells (W1) and 62 ms for strongly biphasic cells (W3). Even though the example neurons shown in Fig. 1, *A* and *B,* show similar temporal extent, in general, the strongly biphasic profile covers a longer time period than the weakly biphasic one. Direction reversals thus require additional time, but are initiated early on. We checked whether several parameters, such as FSS, Δ*t*, W1, W2, and W3 (for explanation of these terms see Table 1), varied systematically with the value of the biphasic index. The only parameter that clearly varied with the biphasic index across the total population was the duration of the main peak in the reverse correlogram (W1), defined as the time difference between first and last "significant" positive excursion for the preferred direction. This duration decreased significantly with increasing levels of the biphasic index, for the total population, and for the weakly biphasic group. For strongly biphasic cells, however, no such dependency was found. The conclusion one can draw from these results is that the temporal dynamics of the short latency response (W1) changes due to the long latency response of cells with biphasic behavior. In the analysis described above, the reverse correlograms were smoothed with a Gaussian sliding window average with an SD of 8 ms. Using a running window average with a smaller SD (4 ms) gives similar results, except that W1 is not significantly correlated to the biphasic index for the weakly biphasic group ($r = -0.05$).

Biphasic temporal profile and short-term adaptation

Neurons in area MT respond to continuously moving stimuli with a transient-sustained firing pattern. This phenomenon, called short-term adaptation, is characterized by a vigorous

response to the initial part of the stimulus settling rapidly to a lower firing rate (Priebe and Lisberger 2002; Priebe et al. 2002).

To study the relation between biphasic response and short-term adaptation, we recorded the responses of 31 neurons to continuously moving random dot patterns in the preferred direction. To describe the short-term adaptation strength of the resulting histograms, we fit the transition from transient to sustained firing rate with single exponentials similarly to that described by Priebe and Lisberger (2002) according to the form

$$R(t) = f_{sus} + (f_{trans} - f_{sus})e^{-t/k} \quad (2)$$

where f_{sus} is the firing rate during the sustained part of the response, f_{trans} is the initial transient level of the response, and k is the time constant of the exponential.

Using the parameters from the fits, short-term adaptation strength was defined as the ratio of transient/sustained response level (*TSR*) as

$$\mathrm{TSR} = f_{trans}/f_{sus} \quad (3)$$

Figure 4 shows the transient/sustained ratio of these 31 neurons plotted against their biphasic indices. The figure shows no correlation between the biphasic behavior and adaptation strength (the r value of the linear fit was 0.23, $P > 0.05$). This indicates that biphasic responses are probably not due to the same short-term adaptation mechanism that determines the degree of transience in MT cell responses.

Second-order analysis of successive motion directions

We showed that a substantial proportion of MT neurons has a biphasic temporal direction tuning profile, which is associated with a reversal of direction preference. In nearly all cells, the preferred direction corresponded to the peak in the short latency phase and the antipreferred direction to the peak in the second phase (at a longer latency). This finding suggests that the optimal stimulus for a neuron with biphasic characteristics is a change of stimulus direction, from antipreferred to preferred direction. From the results presented so far, it is not clear whether biphasic behavior is an inherent property of the cell's response to a single step or results from specific combinations of stimuli, e.g., a step in the antipreferred direction followed by the preferred direction.

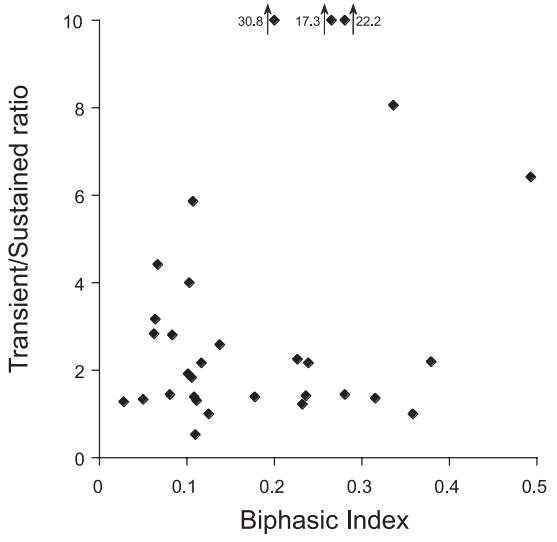

FIG. 4. Biphasic behavior is not correlated with short-term adaptation. Neurons ($n = 31$) were recorded both with a motion reverse correlation paradigm and a continuously moving random dot display. Continuously moving stimuli were presented in the preferred direction for a duration of 1 s and were repeated 10 times. Other parameters of the long-duration stimuli were identical with the motion reverse correlation stimulus. Transient/sustained ratio indicates the strength of adaptation to a continuously moving pattern. Each symbol indicates 1 neuron. The r value of the linear fit was 0.23 ($P > 0.05$). Three extreme outliers are plotted at the *top*. Their corresponding transient/sustained ratios are indicated next to the arrows.

To investigate the contribution of specific combinations of motion directions on the correlograms, we performed a second-order analysis on the data. While the first-order analysis examines the effect of a single direction on the cell response, second-order reverse correlograms represent the probability of a particular stimulus-combination preceding the spikes. The two stimuli can be consecutive or separated in time by one or more stimuli. Unless stated otherwise, we based the second-order analysis on consecutive stimuli.

The response probabilities over time of 64 (8^2) possible combinations of motion directions are shown in Fig. 5. For the explanation of Fig. 5, it is important to note several things. First, a spike is correlated to the occurrence of the *second* presented motion step in the combination. The white spot from about 40 to 70 ms in the middle vertical panel of Fig. 5*A* (indicated by the white arrow) is due to the response to the preferred direction, when it was the second stimulus in the combination. The effect of the first stimulus arrives earlier than the second stimulus. Since the first stimulus is coupled to the second one, the effect will appear in the correlograms before the second stimulus. The parallel white stripes in each panel from 20 to 40 ms correspond to the response to the preferred direction when it was the *first* stimulus in the stimulus pair. Latency differences between the first response (~30 ms) and the second response (~60 ms) are directly related to the motion step delay (in this case 27 ms; 2 frames at a monitor refresh rate of 75 Hz). The second-order reverse correlogram of the neuron with low biphasic index in Fig. 5*A* shows that probability levels are highest for the preferred/preferred combination. Probabilities decrease as the first stimulus deviates from the preferred direction. This reflects that combinations of successive steps in the preferred direction have the highest probability of evoking spikes. We find similar probability patterns for the group of cells with a low biphasic index.

Figure 5*B* shows the second-order reverse correlograms for an example cell with a high biphasic index. In contrast to the previous example in Fig. 5*A*, this neuron has the highest probability for an antipreferred/preferred stimulus combination. Other high probabilities occur in this cell for the +135/−45 and the −135/+45 combinations, as indicated by the white arrows in Fig. 5*B*. Generally, neurons with a high biphasic index showed probability patterns with a preference to the antipreferred/preferred directional change. This is exactly what was already suggested by the first-order plot in Fig. 1*B*, e.g., these neurons respond most optimally to a directional reversal from antipreferred to preferred. Figure 5*B* also shows that these effects are highly directionally specific. If the second stimulus in the combination deviates ±45° from the preferred direction, the most optimal direction preceding it is not the antipreferred direction, but rather a direction differing by 180°.

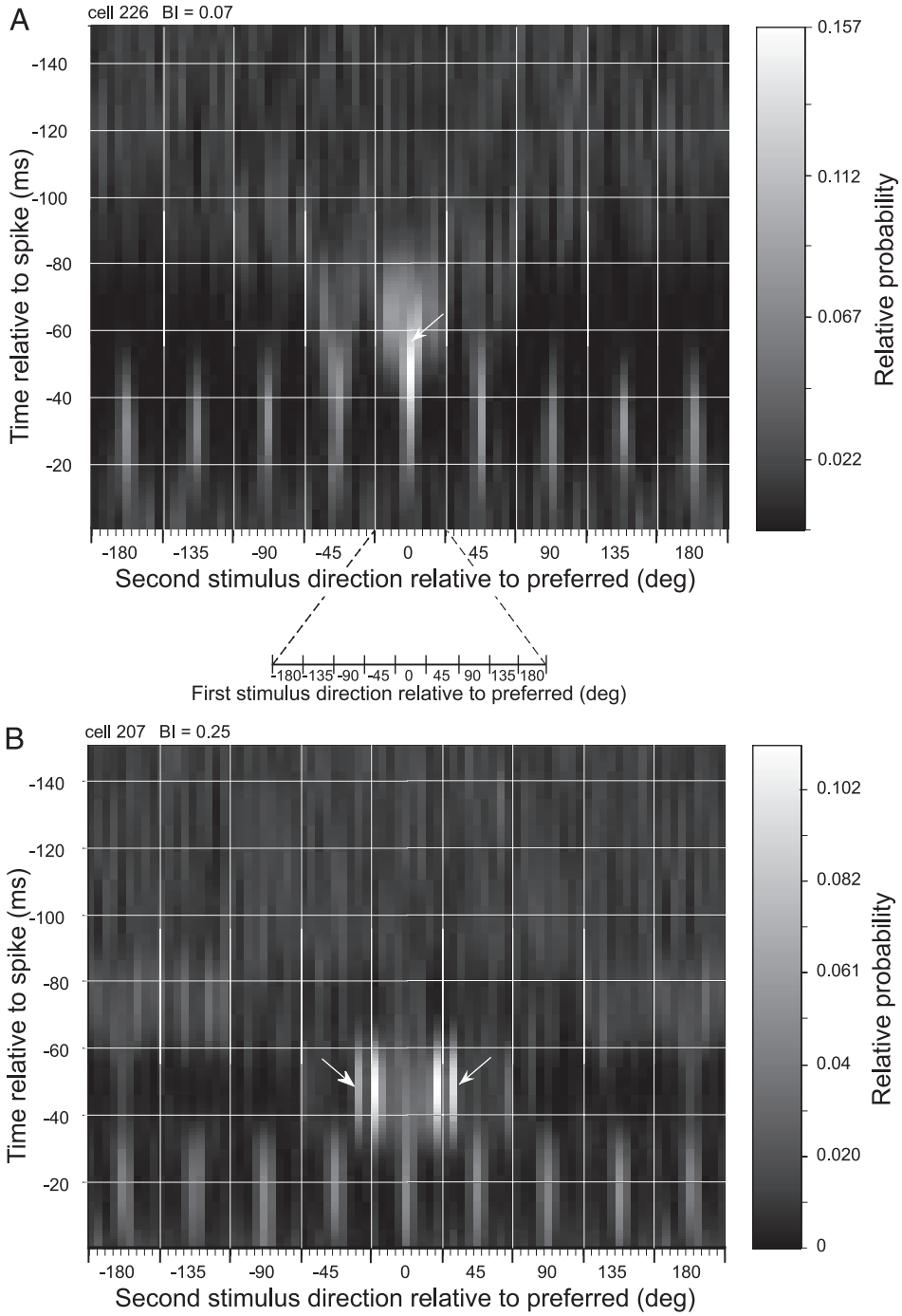

FIG. 5. Effect of stimulus combinations on response. Second-order reverse correlograms show 64 possible combinations of 2 stimulus directions. *A*: an example neuron with a low biphasic index (BI = 0.07). *B*: an example neuron with a high biphasic index (BI = 0.25). Each panel in these figures comprises 9 columns representing the relative direction of the 2nd stimulus of a sequence. Nested within each of these columns are 9 smaller columns representing the relative direction of the 1st stimulus in a pair of motion directions. Directions are relative to the preferred direction; +180 and −180° stimuli are identical. Dark shading indicates low probability; white spots indicate high probabilities. Spikes are correlated to the 2nd element of the stimulus combination. Correlograms were smoothed with a Gaussian profile (SD, 8 ms). White arrow in *A* indicates a high probability for a preferred/preferred (0/0°) stimulus combination. White arrows in *B* indicate high probability for +135/−45, +180/0, and −135/+45° stimulus combinations.

The second-order analysis for the cell in Fig. 5*B* was performed for two consecutive motion steps with a temporal interval of 27 ms, which is almost equal to Δt (29 ms) as described in the first-order analysis (Table 1). However, for a substantial number of neurons, Δt is in the order of two or more motion step durations. For these neurons, second-order reverse correlograms show increased activity for stimulus combinations separated by time intervals longer than one motion step duration. For successive combinations of stimuli, these neurons behaved much like the monophasic neurons, showing a preference to preferred/preferred combination. Results for combinations of motion steps thus seem to agree qualitatively to what one would predict from combining the profiles for the separate stimuli. We will investigate whether profiles for individual motion steps predict profiles for motion step combinations quantitatively.

Nonlinear interactions between successive motion directions

To quantitatively test predictions for second-order correlograms (combinations of motion steps) from first-order profiles (individual motion steps), we multiplied two first-order reverse correlograms and compared the result to the second-order reverse correlograms. Because reverse correlograms reflect probabilities, multiplying two individual correlograms predicts the probability for their combination to occur. (Note that this is

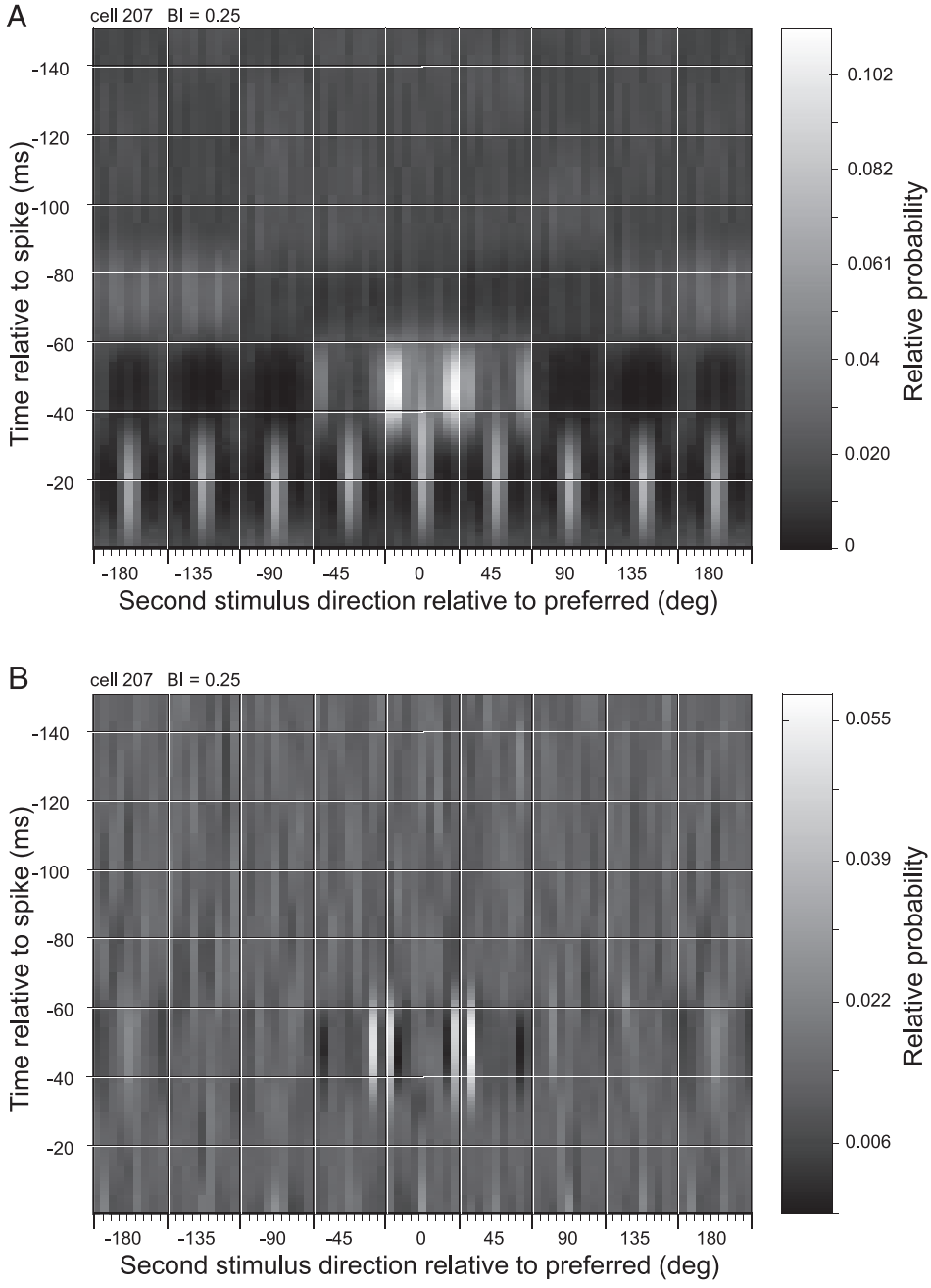

FIG. 6. Linear analysis of the 2nd-order reverse correlation. *A*: predicted 2nd-order reverse correlograms based on individual 1st-order correlograms. Predictions were obtained by multiplying 2 1st-order correlograms. *B*: prediction errors of 2nd-order reverse correlograms for the example cell shown in *A* and Fig. 5*B*. Prediction errors show the difference between measured correlograms (Fig. 5*B*) and linear predictions (*A*). Conventions are similar to Fig. 5, *A* and *B*. Positive errors (light) represent stimulus probabilities that are underestimated (prediction is lower than observed), whereas negative errors (dark) represent probabilities that are overestimated (prediction is higher than the observed response).

similar to summing the responses when responses would be expressed as firing rates). Since the first stimulus occurs earlier, its reverse correlogram was shifted in time by the duration of one motion step. Differences between measured and predicted second-order profiles indicate direction-specific temporal interactions in the response of MT neurons. Predicted and measured responses for all possible combinations of directions were compared.

Figure 6*A* shows the predicted second-order reverse correlograms for the same cell whose measured second-order reverse correlogram is shown in Fig. 5*B*. The predicted correlograms are less noisy due to the fact that first-order reverse correlograms are based on a larger number of stimulus occurrences than second-order correlograms (a factor of 8). The fact that correlograms for specific combinations of directions are well described by predictions based on the individual directions shows that the typical biphasic behavior does not result from specific stimulus combinations.

To visualize the differences between the two figures, we subtracted the predicted second-order reverse correlograms from the measured second-order reverse correlograms (Fig. 5*B* − Fig. 6*A* = Fig. 6*B*). The remaining prediction errors reveal nonlinear interactions between specific motion directions. White spots in Fig. 6*B* show combinations for which the actual correlation was higher than that predicted from the individual directions. This example cell shows responses that are larger than predicted (white color) for stimulus combinations of antipreferred/preferred, 135/−45°, and −135/45°, and decreased responses (black color) for −135/−45, −135/0, 135/0, and 135/45°.

To explore the relationship between the biphasic response profile and the level of nonlinearity, we plotted the biphasic index of each neuron against the prediction errors for antipreferred/preferred and preferred/preferred stimulus combinations. On average, the largest prediction errors were found 6 ms before the peak latency. For this reason, we calculated the average prediction error at an 11-ms-period around this most informative part centered around 6 ms prior to peak latency. The average prediction error of this 11-ms-long period for antipreferred/preferred and preferred/preferred stimulus combinations is shown in Fig. 7.

Neither antipreferred/preferred prediction errors nor preferred/preferred prediction errors showed significant correlation with the biphasic index (r values were 0.08 and 0.01, respectively, $P > 0.05$ for both cases). If specific directional interactions contributed significantly to the biphasic temporal response profile, we would expect a relationship between the biphasic index and the level of nonlinearity. The most important conclusion from this analysis is that biphasic behavior does not result from specific sequences of stimuli. Therefore it is probably an inherent property of the cell's response to a single motion step. The prediction errors for antipreferred/preferred combinations were on average positive (0.03 ± 0.08), indicating larger responses, whereas the mean prediction error for the preferred/preferred stimulus combination was negative (-0.08 ± 0.1), indicating lower responses as expected from linear summation. Furthermore, prediction errors for the antipreferred/preferred combination were significantly higher than those for the preferred/preferred combinations (paired t-test, $P < 0.01$).

Similarly, as we calculated the mean prediction error for antipreferred/preferred and preferred/preferred combinations, we calculated the mean prediction error for all combinations of directions. These averages summarize nonlinear interactions between successive stimuli over the entire population (Fig. 8A). On average, the largest negative prediction error occurred for the preferred/preferred combination (black color). This indicates that, for this combination, the prediction is higher than the measured response. Positive prediction errors were observed for 180, 135, and 90° directional changes (dark color), irrespective of the preferred direction. The average prediction error was 14% for the preferred/preferred second-order reverse correlogram and 10% for the antipreferred/preferred second-order reverse correlogram. In general, neurons had similar interaction patterns except that the strongly biphasic neurons showed somewhat larger prediction errors. The

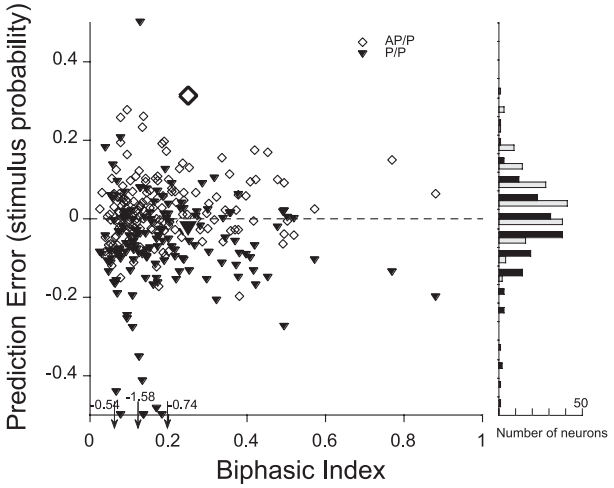

FIG. 7. Biphasic behavior is not due to specific nonlinear interactions between successive stimuli. Relationship between the biphasic index and the level of nonlinearity for antipreferred/preferred (AP/P) and preferred/preferred (P/P) combination. Each neuron contributes to 2 symbols in this figure. Enlarged triangle and diamond indicate example cell 207 (same as Figs. 5B and 7). Three extreme outliers are plotted at the *bottom*. Their corresponding prediction error values are indicated next to the arrows. The r value of a linear fit for AP/P and P/P combination was 0.08 and 0.01, respectively ($P > 0.05$ for both cases).

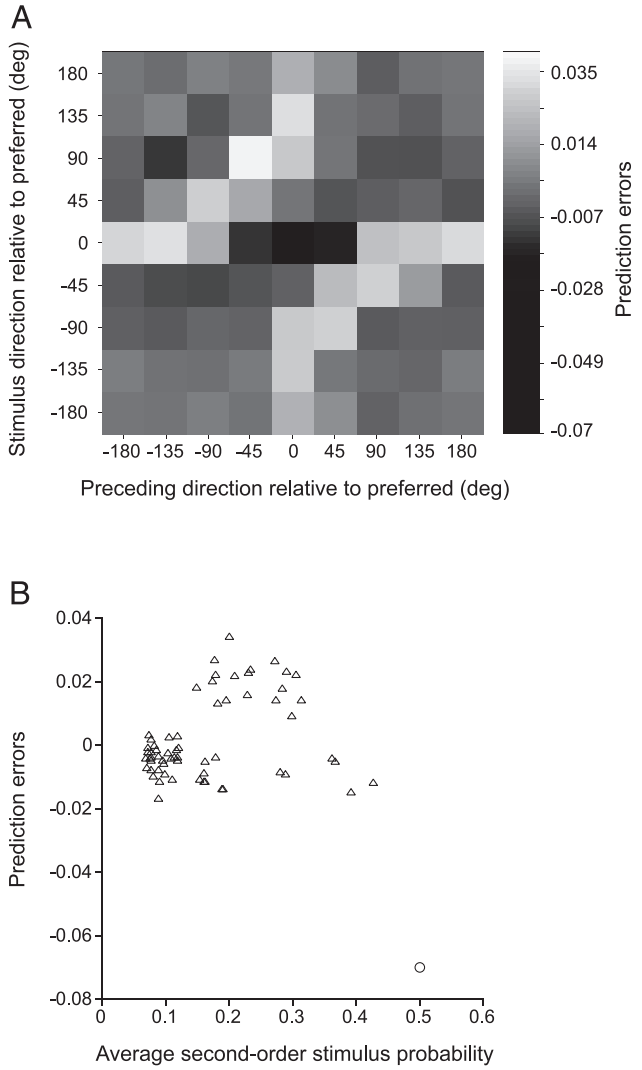

FIG. 8. Prediction errors for different combinations of stimulus directions. For each combination of 2 consecutive directions, prediction errors were averaged over the whole population. Average prediction error of an 11-ms-long section (centered at 6 ms prior to response latency) is shown. A: negative interactions occur for P/P stimulus combination and positive interactions between near opposing stimuli (180, 135, and 90° change). Shading indicates negative interactions (response probability is lower than the linear prediction), and light colors indicate positive interactions (response probability is higher than linear prediction). Color scale of the figure is logarithmic to visualize positive interactions between stimulus combinations with angular differences of near 180°. Same data are represented in a linear way in B. B: prediction errors as shown in A plotted as a function of the average 2nd-order stimulus probability level at the same time segment of correlograms. Each symbol represents a combination of 2 consecutive motion directions. Open circle represents the P/P combination.

prediction error for preferred/preferred combination was 11% in the weakly biphasic group and 20% in the strongly biphasic group. For the antipreferred/preferred combination, it was 6% in the weakly biphasic group and 14% in the strongly biphasic group.

The prediction error for the preferred/preferred combination can be explained by a simple static nonlinearity at the output of the neuron. If a preferred stimulus follows a preferred stimulus, the neuron responds less than the sum of the two responses due to saturation. However, for opposite motion directions, the responses are higher than predicted, which cannot be explained by a static nonlinearity at the output of the neuron. In Fig. 8*B,* the average prediction error for the cell population is plotted against the average second-order stimulus probabilities. This plot shows that only specific combinations of directions show prediction errors and that prediction error is not correlated with the absolute probability level. The prediction errors for specific (nearly) opposite combinations of directions are therefore not the result of a static nonlinearity at the output of the neuron but could reflect for instance specific network interactions before or within MT.

In the analysis described above, we investigated the effect of successive stimulus combinations on the response. It is also possible to investigate the effect of stimulus combinations, which are separated in time by other stimuli. To this end, we analyzed the level of nonlinearity for increasing temporal separation. For this analysis, we chose 11 strongly biphasic neurons with a Δt around 24 ms (duration of 3 motion steps). We computed the prediction errors for each cell for the temporal separation of one, two, three, or four motion steps between stimuli (separation of 1 motion step means successive stimulus combinations). We found decreasing prediction errors in all cases, as the temporal separation between the stimulus combinations increased, suggesting that the strongest nonlinearity occurs between successive stimuli. If biphasic profiles were due to nonlinear interactions between specific motion steps separated by Δt, we would expect the strongest nonlinearity for these neurons at the temporal separation of three motion steps. Since this is not the case, these results support the conclusion that biphasic behavior does not result from the specific nonlinear directional interactions that are shown in Fig. 8*A* for two opposite consecutive motion directions.

DISCUSSION

Biphasic responses

We examined the dynamics of direction tuning and the effect of directional changes at the preferred step size of MT neurons. The temporal profiles of the reverse correlograms, describing relative responses to individual motion steps at different directions, showed different degrees of biphasic behavior. Preferred directions for neurons with a low biphasic index did not change over time. Direction tuning of neurons with a high biphasic index, on the other hand, showed a directional change from antipreferred to preferred direction over time.

Reversal effects are a common feature of reverse correlograms and have been described in different visual areas, i.e., for luminance contrast reverse correlograms of neurons in the retina (Rowe and Palmer 1995), lateral geniculate nucleus (Cai et al. 1997; Reid et al. 1991, 1997), and primary visual cortex (DeAngelis et al. 1995; DeValois et al. 2000; Dragoi et al. 2002; Mazer et al. 2002; Reid et al. 1991; Ringach et al. 1997, 2003). A substantial fraction of motion-sensitive neurons in area MT can have similar biphasic correlograms in the motion domain, as is shown by our results and other recent work (Bair and Movshon 2004; Bair et al. 2002). However, a recent report by Cook and Maunsell (2004) reports only a very small fraction of MT neurons with biphasic behavior. The question arises how these differences in degree of biphasic behavior can be explained.

Possible explanations for differences in biphasicness could be related to known differences in MT cell spatial response characteristics like center-surround organization and "plaid" versus "component" responses (Allman et al. 1985; Born 2000; Movshon et al. 1985; Rodman and Albright 1989; Xiao et al. 1995). Further investigation would be necessary to establish whether such a correlation exists. Most probably more important factors that determine the degree of biphasicness are stimulus attributes like spatial frequency, temporal frequency, speed, contrast, etc. Some reports (Bair and Movshon 2004; Bair et al. 2002) indeed show that speed, spatial frequency, and contrast can change the shape of the reverse correlogram. This could also be the explanation why Cook and Maunsell (2004) hardly found any biphasic neurons in their sample of MT neurons, since their stimulus (dynamic noise) was different from the stimulus we used (field movement impulse stimulus). Our results show that the phase reversal of the correlograms occurs simultaneously for all directions. Furthermore, the peak latencies of the first and second phase of reverse correlograms for different directions are similar. This indicates that probabilities for different directions change with similar dynamics.

Priebe and colleagues (Priebe and Lisberger 2002; Priebe et al. 2002) have intensively investigated short-term adaptation in MT neurons that is related to transient responses. At first sight our results on biphasic responses seem to be correlated with short-term adaptation. A biphasic profile for individual responses would predict effects similar to short-term adaptation, with vigorous responses to the initial part of the stimulus settling rapidly to a lower firing rate. Similar to the distribution of adaptation strength reported by Priebe and Lisberger, we find a wide, unimodal distribution for the biphasic effect. However, we do not find a correlation with the transient behavior of the neurons. This indicates that biphasic responses are not due to the same short-term adaptation mechanism that determines the degree of transience in MT cell responses.

Weak and strong biphasic characteristics seem to correspond well to different requirements for motion-sensitive cells tuned for either optimal temporal integration or segregation. To construct a useful representation of moving patterns in the outside world, two mechanisms always compete. Sometimes motion directions need to be integrated over time to detect the overall flow of moving objects. On the other hand, motion direction differences need to be segmented to distinguish differently moving objects. Our results show that the competition between temporal motion integration and segregation is reflected in responses to single motion steps, at the level of MT.

Second-order characteristics

We examined temporal interactions by measuring the effect of combinations of successive stimuli in eight different directions. Weakly biphasic cells showed an increased firing probability for a motion step, after a preceding step in the preferred direction. Strongly biphasic cells, on the other hand, showed a decreased firing probability after a preceding step in the preferred direction. This is in accordance with previous reports that show that the response to the preferred direction strongly depends on the preceding motion direction (Bair et al. 2002; Priebe and Lisberger 2002; Priebe et al. 2002). Stimulation with the preferred direction decreases the response to a successive preferred direction (short-term adaptation), and stimulation with the antipreferred direction either decreases or increases the responses to successive preferred directions.

The comparison of correlograms for specific combinations to the correlograms for individual motion steps shows that, to a large extent, they follow from the profiles for individual steps through simple linear summation. In addition, we also found evidence for "nonlinear," directionally specific interactions. Prediction errors for the second-order reverse correlograms clearly showed two different types of nonlinear interactions. First, we found negative prediction errors (a lower response than predicted) for successive presentations of motion steps in the preferred direction. This might either reflect short-term adaptation or a saturation type of nonlinearity. The second, more interesting, nonlinear interaction that we found was positive prediction errors for antipreferred/preferred combinations (facilitation). This effect was found both for weakly and strongly biphasic neurons and did not correlate with the biphasic index. The facilitation is in line with interactions along the preferred-antipreferred axis described previously (Bair et al. 2002; Priebe and Lisberger 2002; Priebe et al. 2002). Our results for different combinations of directions, furthermore, show that similar facilitatory effects are also found for combinations other than preferred and antipreferred, as long as they differ by about 180° deg (facilitation to near opposing directions). Facilitation was observed for directional changes of about 180°, irrespective of a cell's preferred direction. The directionally specific interactions that we found were not related to the activity level of a cell and therefore cannot be due to a simple static nonlinearity at the output of MT neurons.

The observed facilitatory interactions for near opposite directions are not consistent with a divisive normalization model, as proposed by several studies, to account for spatial integration in MT (Britten and Heuer 1999; Simoncelli and Heeger 1998). In divisive normalization models, the gain of the output of a single MT neuron is set by the average activity of all MT neurons tuned to different directions. Such models can account for the fact that the firing rate to a combination of two stimuli in the receptive field presented simultaneously is predicted by the average of the responses when they are presented separately (Britten and Heuer 1999; Britten and Newsome 1990; Ferrera and Lisberger 1997; Recanzone et al. 1997). This model cannot account for the temporal integration effects found in our study, because the effect is directionally specific and not global, and because normalization would lead to decreased activity rather than facilitation. Furthermore, we find the largest nonlinear interactions on average 6 ms before the peak of the response. It is unlikely that normalization would peak even before the maximum response level is achieved. The simplest model to account for our data would be specific facilitatory input from oppositely tuned combinations of motion sensitive neurons for all motion directions at the input of MT, for instance from V1.

Our results show that area MT neurons are generally more responsive when sudden changes in motion directions occur, irrespective of the preferred direction of the neurons. This specific nonlinear mechanism might play an important role in signaling relevant changes in the pattern of motion and provide additional information for directing eye movements and attracting attention to interesting parts of the visual field.

ACKNOWLEDGMENTS

We thank I. Vajda for helpful discussions and providing parts of the analysis software, P. Sterling for useful comments on earlier drafts of the manuscript, and T. Stuivenberg and the other technicians of our laboratory for technical support.

GRANTS

This study was supported by the Innovational Research Incentives Scheme of the Netherlands Organization for Scientific Research and the Interuniversity Attraction Poles Programme of the Belgian Science Policy.

REFERENCES

Albright TD. Direction and orientation selectivity of neurons in visual area MT of the macaque. *J Neurophysiol* 52: 1106–1130, 1984.

Allman J, Miezin F, and McGuinness E. Direction- and velocity-specific responses from beyond the classical receptive field in the middle temporal visual area (MT). *Perception* 14: 105–126, 1985.

Bair W, Cavanaugh JR, Smith MA, and Movshon JA. The timing of response onset and offset in macaque visual neurons. *J Neurosci* 22: 3189–3205, 2002.

Bair W and Movshon JA. Adaptive temporal integration of motion in direction-selective neurons in macaque visual cortex. *J Neurosci* 24: 9305–9323, 2004.

Borghuis BG, Perge JA, Vajda I, van Wezel RJA, van de Grind WA, and Lankheet MJM. The motion reverse correlation (MRC) method: a linear systems approach in the motion domain. *J Neurosci Methods* 123: 153–166, 2003.

Born RT. Center-surround interactions in the middle temporal visual area of the owl monkey. *J Neurophysiol* 84: 2658–2669, 2000.

Born RT and Tootell RB. Segregation of global and local motion processing in primate middle temporal visual area. *Nature* 357: 497–499, 1992.

Britten KH and Heuer HW. Spatial summation in the receptive fields of MT neurons. *J Neurosci* 19: 5074–5084, 1999.

Britten KH and Newsome WT. Responses of MT neurons to discontinuous motion stimuli. *Invest OpthmalVis Sci Suppl* 31: 238, 1990.

Britten KH and Newsome WT. Tuning bandwidths for near-threshold stimuli in area MT. *J Neurophysiol* 80: 762–770, 1998.

Britten KH, Newsome WT, Shadlen MN, Celebrini S, and Movshon JA. A relationship between behavioral choice and the visual responses of neurons in macaque MT. *Vis Neurosci* 13: 87–100, 1996.

Britten KH, Shadlen MN, Newsome WT, and Movshon JA. The analysis of visual motion: a comparison of neuronal and psychophysical performance. *J Neurosci* 12: 4745–4765, 1992.

Buracas GT, Zador AM, DeWeese MR, and Albright TD. Efficient discrimination of temporal patterns by motion-sensitive neurons in primate visual cortex. *Neuron* 20: 959–969, 1998.

Cai D, DeAngelis GC, and Freeman RD. Spatiotemporal receptive field organization in the lateral geniculate nucleus of cats and kittens. *J Neurophysiol* 78: 1045–1061, 1997.

Cook EP and Maunsell JH. Attentional modulation of motion integration of individual neurons in the middle temporal visual area. *J Neurosci* 24: 7964–7977, 2004.

DeAngelis GC, Ohzawa I, and Freeman RD. Receptive-field dynamics in the central visual pathways. *Trends Neurosci* 18: 451–458, 1995.

De Valois RL, Cottaris NP, Mahon LE, Elfar SD, and Wilson JA. Spatial and temporal receptive fields of geniculate and cortical cells and directional selectivity. *Vision Res* 40: 3685–3702, 2000.

Dragoi V, Sharma J, Miller EK, and Sur M. Dynamics of neuronal sensitivity in visual cortex and local feature discrimination. *Nat Neurosci* 5: 883–891, 2002.

Dubner R and Zeki SM. Response properties and receptive fields of cells in an anatomically defined region of the superior temporal sulcus in the monkey. *Brain Res* 35: 528–532, 1971.

Ferrera VP and Lisberger SG. Neuronal responses in visual areas MT and MST during smooth pursuit target selection. *J Neurophysiol* 78: 1433–1446, 1997.

Heuer HW and Britten KH. Contrast dependence of response normalization in area MT of the rhesus macaque. *J Neurophysiol* 88: 3398–3408, 2002.

Julesz B. *Foundations of Cyclopean Perception.* Chicago, IL: University of Chicago Press, 1971.

Lisberger SG and Movshon JA. Visual motion analysis for pursuit eye movements in area MT of macaque monkeys. *J Neurosci* 19: 2224–2246, 1999.

Livingstone MS, Pack CC, and Born RT. Two-dimensional substructure of MT receptive fields. *Neuron* 30: 781–793, 2001.

Malpeli JG. Measuring eye position with the double magnetic induction method. *J Neurosci Methods* 86: 55–61, 1998.

Maunsell JH and Van Essen DC. Functional properties of neurons in middle temporal visual area of the macaque monkey. I. Selectivity for stimulus direction, speed, and orientation. *J Neurophysiol* 49: 1127–1147, 1983.

Mazer JA, Vinje WE, McDermott J, Schiller PH, and Gallant JL. Spatial frequency and orientation tuning dynamics in area V1. *Proc Natl Acad Sci USA* 99: 1645–1650, 2002.

Mikami A, Newsome WT, and Wurtz RH. Motion selectivity in macaque visual cortex. I. Mechanisms of direction and speed selectivity in extrastriate area MT. *J Neurophysiol* 55: 1308–1327, 1986.

Movshon JA, Adelson EH, Gizzi MS, and Newsome WT. The analysis of moving visual patterns. In: *Study Group on Pattern Recognition Mechanisms,* edited by Chagas C, Gattass R, and Gross C. Vatican City: Pontifica Academia Scientiarum, 1985, p. 117–151.

Newsome WT and Paré EB. A selective impairment of motion perception following lesions of the middle temporal visual area (MT). *J Neurosci* 8: 2201–2211, 1988.

Pack CC, Berezovskii VK, and Born RT. Dynamic properties of neurons in cortical area MT in alert and anaesthetized macaque monkeys. *Nature* 414: 905–908, 2001.

Pack CC and Born RT. Temporal dynamics of a neural solution to the aperture problem in visual area MT of macaque brain. *Nature* 409: 1040–1042, 2001.

Pack CC, Gartland AJ, and Born RT. Integration of contour and terminator signals in visual area MT of alert macaque. *J Neurosci* 24: 3268–3280, 2004.

Priebe NJ, Churchland MM, and Lisberger SG. Constraints on the source of short-term motion adaptation in macaque area MT. I. The role of input and intrinsic mechanisms. *J Neurophysiol* 88: 354–369, 2002.

Priebe NJ and Lisberger SG. Constraints on the source of short-term motion adaptation in macaque area MT. II. Tuning of neural circuit mechanisms. *J Neurophysiol* 88: 370–382, 2002.

Raiguel S, Van Hulle MM, Xiao DK, Marcar VL, and Orban GA. Shape and spatial distribution of receptive fields and antagonistic motion surrounds in the middle temporal area (V5) of the macaque. *Eur J Neurosci* 7: 2064, 1995.

Recanzone GH, Wurtz RH, and Schwarz U. Responses of MT and MST neurons to one and two moving objects in the receptive field. *J Neurophysiol* 78: 2904–2915, 1997.

Reid RC, Soodak RE, and Shapley RM. Directional selectivity and spatiotemporal structure of receptive fields of simple cells in cat striate cortex. *J Neurophysiol* 66: 505–529, 1991.

Reid RC, Victor JD, and Shapley RM. The use of m-sequences in the analysis of visual neurons: linear receptive field properties. *Vis Neurosci* 14: 1015–1027, 1997.

Reulen JP and Bakker L. The measurement of eye movement using double magnetic induction. *IEEE Trans Biomed Eng* 29: 740–744, 1982.

Ringach DL, Hawken MJ, and Shapley R. Dynamics of orientation tuning in macaque V1: the role of global and tuned suppression. *J Neurophysiol* 90: 342–352, 2003.

Ringach DL, Sapiro G, and Shapley R. A subspace reverse-correlation technique for the study of visual neurons. *Vision Res* 37: 2455–2464, 1997.

Rodman HR and Albright TD. Single-unit analysis of pattern-motion selective properties in the middle temporal visual area (MT). *Exp Brain Res* 75: 53–64, 1989.

Rowe MH and Palmer LA. Spatio-temporal receptive-field structure of phasic W cells in the cat retina. *Vis Neurosci* 12: 117–139, 1995.

Rudolph K and Pasternak T. Transient and permanent deficits in motion perception after lesions of cortical areas MT and MST in the macaque monkey. *Cereb Cortex* 9: 90–100, 1999.

Salzman CD, Murasugi CM, Britten KH, and Newsome WT. Microstimulation in visual area MT: effects on direction discrimination performance. *J Neurosci* 12: 2331–2355, 1992.

Simoncelli EP and Heeger DJ. A model of neuronal responses in visual area MT. *Vision Res* 38: 743–761, 1998.

Snowden RJ, Treue S, Erickson RG, and Andersen RA. The response of area MT and V1 neurons to transparent motion. *J Neurosci* 11: 2768–2785, 1991.

Treue S, Hol K, and Rauber HJ. Seeing multiple directions of motion-physiology and psychophysics. *Nat Neurosci* 3: 270–276, 2000.

Xiao DK, Raiguel S, Marcar V, Koenderink J, and Orban GA. Spatial heterogeneity of inhibitory surrounds in the middle temporal visual area. *Proc Natl Acad Sci USA* 92: 11303–11306, 1995.